SAND2015-10661C

JOINT DOD/DOE MUNITIONS PROGRAM

Modeling techniques for localization and failure

J. Foulk, K. Karlson, A. Mota, J.T. Ostien, M. Veilleux, J. Emery

2015 TCG-I/XI Fall Meeting
December 8, 2015
Sandia National Laboratory
Albuquerque, NM

Sandia National Laboratories is a multi-program laboratory managed and operated by Sandia Corporation, a wholly owned subsidiary of Lockheed Martin Corporation, for the U.S. Department of Energy's National Nuclear Security Administration under contract DE-AC04-94AL85000.

National Nuclear Security Administration

Sandia National Laboratories

Methods broadly applicable

Goal: Provide techniques for modeling localization and failure that are not mesh dependent to enable predictive simulations of munitions behavior

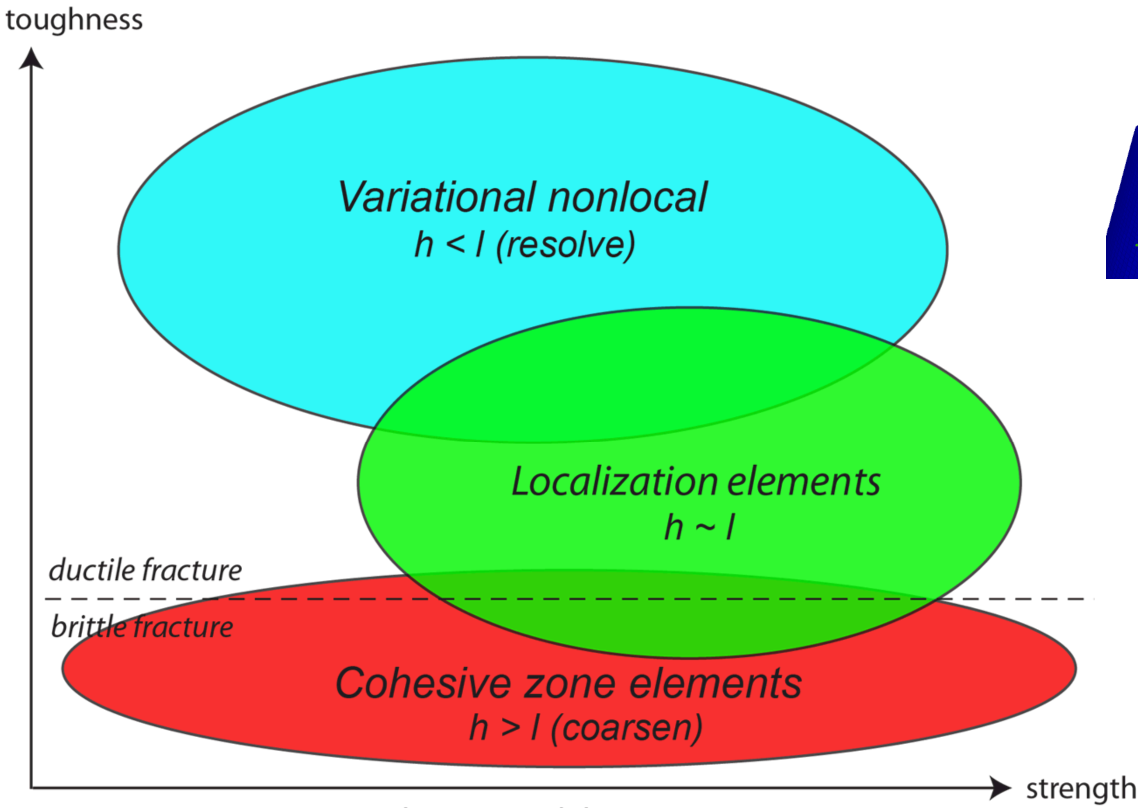

$$l = \text{length scale}_{\text{mode I}} = \frac{\text{toughness} * \text{modulus}}{\text{strength}^2}$$

h = element size

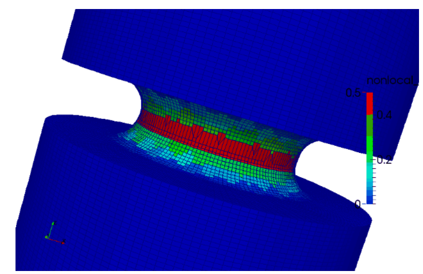

variational nonlocal

localization elements

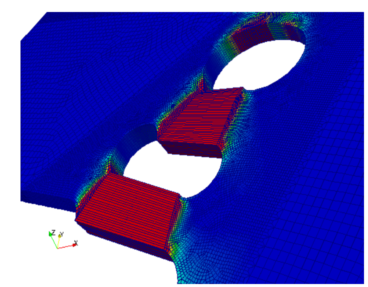

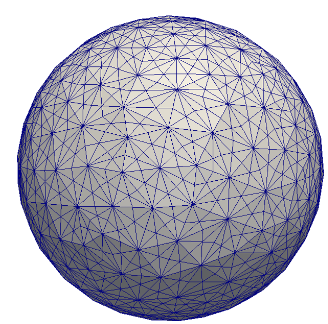

optimal meshes

Changing scope, broadening impact

Task 5, Modeling techniques for localization and failure

- Variational nonlocal method (1.1)
- Localization elements (1.2)
  - Optimal meshes (1.2.1)
  - Adaptive insertion (1.2.2)
  - Linkage to XFEM (1.2.3)

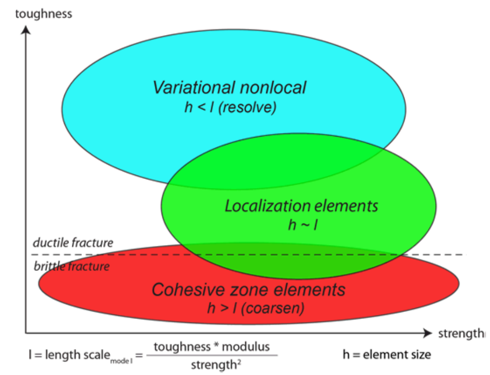

FY16 Deliverable. Demonstration of the adaptive insertion of localization elements on an optimized mesh for mixed-mode fracture. Insertion will be dictated by the bifurcation condition applied to a general class of material models.

FY15 Issue. With the Sierra Toolkit (STK) in flux, we were not able to accommodate the churn in our research environment. We have paused efforts in adaptive insertion to *leverage new work*.

New focus for Task 5, Modeling techniques for localization and failure

- Harden variational nonlocal method and localization elements
- Document work on optimal meshes and the bifurcation condition
- Provide linkage to SierraSM XFEM w/localization elements + insertion criteria
- Leverage efforts to include anisotropy, temperature/rate dependence, damage evolution

Case study - Sandia Fracture Challenge

- Sandia Fracture Challenge (SFC) is a computational challenge for predicting failure open to internal/external competitors
- The second challenge focused on variable rate, mixed-mode crack initiation and propagation in Ti-6Al-4V sheet.
- The challenge announcement included two data sets for material model calibration, geometry information, and test procedures

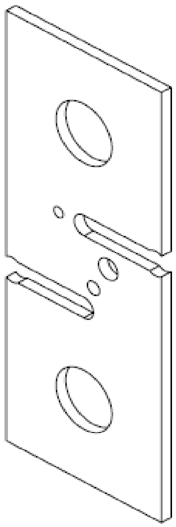

Our approach(s)

- Because Ti-6Al-4V has low thermal conductivity and high strength, one must include thermo-mechanical coupling for the rates of interest.
- Both the provided experimental data and the literature illustrate the need for rate dependence, temperature dependence, anisotropy, and void evolution.
- We leverage a local model with the appropriate phenomenology (micromechanics). We learn about the BVPs through local models.
- We seek to regularize the solution through multiple technologies and understand the space of applicability.

Initial approach to SFC geometry

- Production codes (Sierra) employed for all calculations
- Simulations employ segregated coupling (Adagio/Aria)
- Implicit solution for long time scales (statics & dynamics)
- Isotropic poro-thermo-viscoplasticity model
- Hexahedral elements (SD, constant pressure)
- Pins are fixed
- Element death was employed when the first integration point reached the coalescence criterion ϕ_{coal} (0.15)
- Learn with local damage and coarse meshes
- Employ techniques for regularizing the solution
  - Variational nonlocal method
  - Localization elements

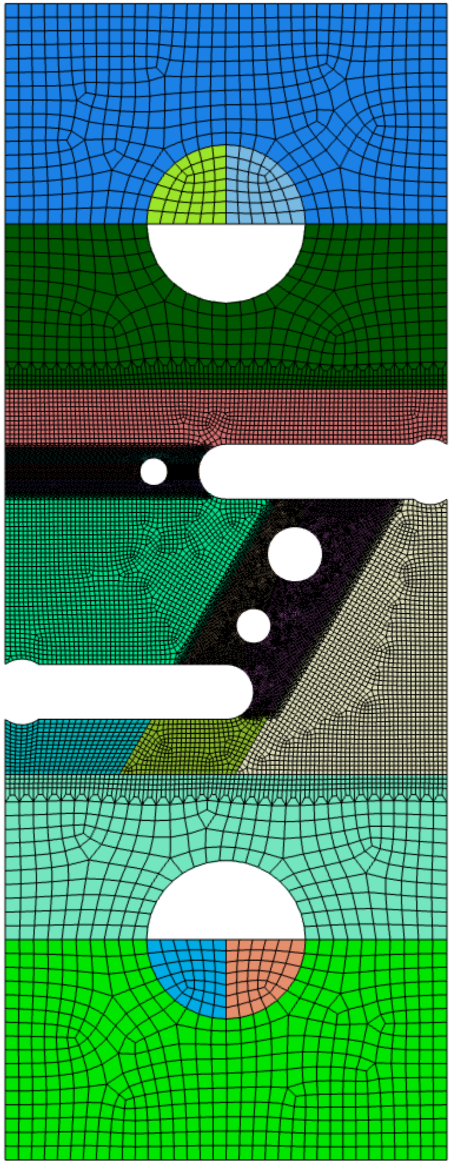

Initial model calibration (tension)

$$\beta = 0.8$$
$$H = 3084 \times 10^6 \text{ (Pa)}$$
$$R_d = 13$$
$$f = 1 \times 10^{-6}$$
$$n = 26$$
$$Y_{RT} = 493 \times 10^6 \text{ (Pa)}$$
$$\phi_0 = 1 \times 10^{-4}$$
$$\phi_{coal} = 0.15$$
$$m = 6$$

Thermo-mechanical simulations employed for model calibration

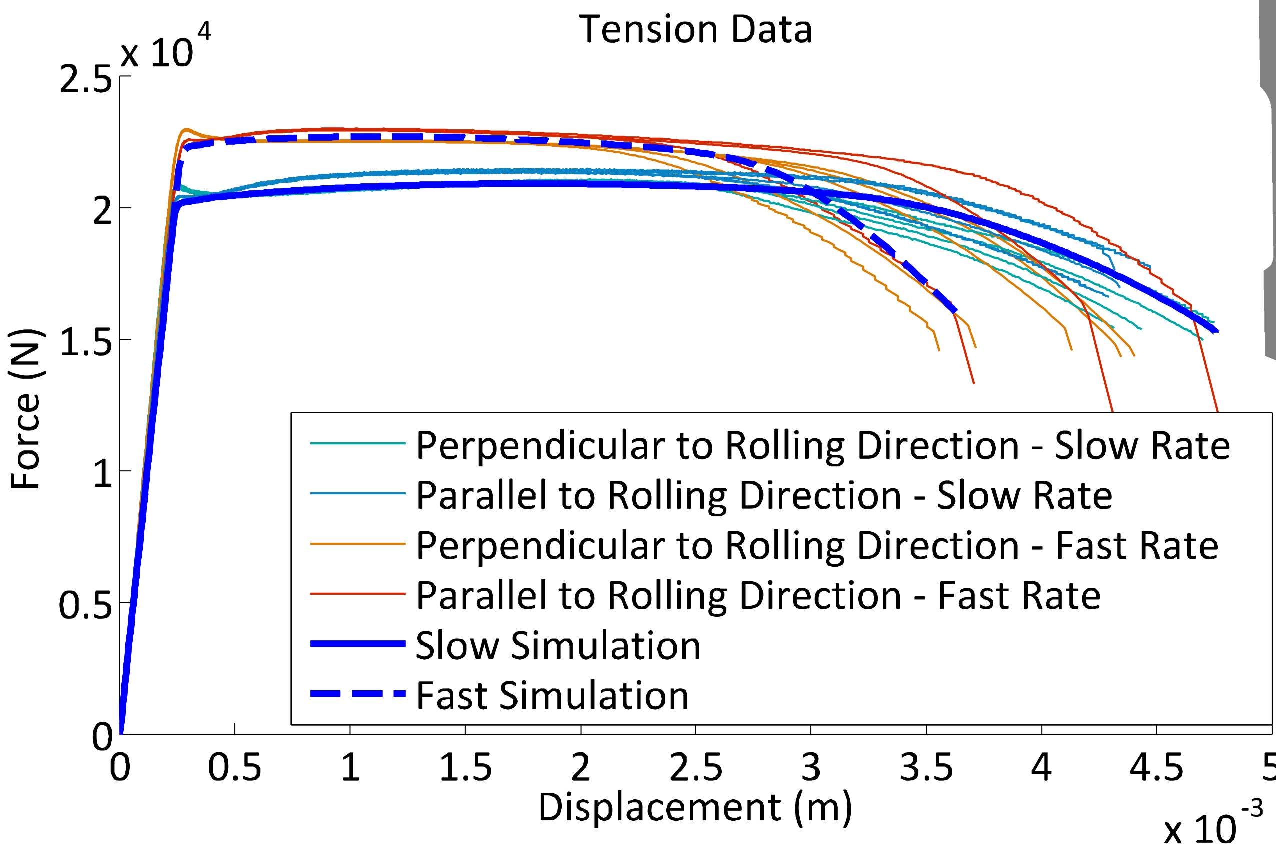

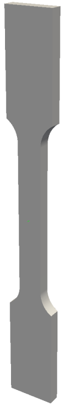

$$\sigma_y = (1-\phi)\left[Y(\theta) + \frac{H}{R_d}\left(1 - e^{-R_d \epsilon_p}\right)\right]\left\{1 + \sinh^{-1}\left[\left(\frac{\dot{\epsilon}_p}{f}\right)^{1/n}\right]\right\}$$

$$\dot{q} = \beta \bar{\boldsymbol{\sigma}} : \boldsymbol{D}^p$$

uncertainty in conversion of plastic work to heat β

$$\dot{\phi} = \sqrt{\frac{3}{2}}\dot{\epsilon}_p \frac{1-(1-\phi)^{m+1}}{(1-\phi)^m} \sinh\left[\frac{2(2m-1)}{2m+1}\frac{\langle \frac{I_1}{3} \rangle}{\sqrt{3J_2}}\right]$$

isotropic damage ϕ taken from Cocks and Ashby (1972)

NOTE: Temperature-dependent thermal conductivity and specific heat also taken from MMPDS-08.

Incorporating shear data

- Calibrated model did not predict the shear behavior
- Anisotropy evident in yield, hardening and damage evolution
- Focused on orientations relevant (// to RD) to the SFC
- Reduced the initial yield Y_{RT} and the recovery R_d
- Incorporated void nucleation through J_3 (n is the evolving void density)

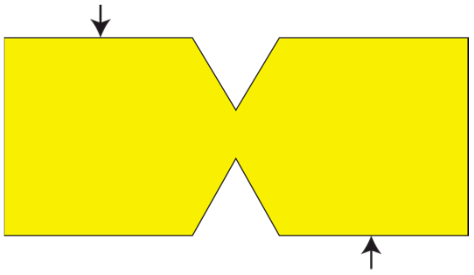

$$\frac{\dot{n}}{n} = N_1 \dot{\epsilon}_p \left(\frac{4}{27} - \frac{J_3^2}{J_2^3} \right)$$

(Horstemeyer, Gokhale, 1999)

$$\frac{\dot{\phi}_n}{\phi} = k_w \dot{\epsilon}_p \left(1 - \frac{27 J_3^2}{4 J_2^3} \right)$$

(Nahshon, Hutchinson, 2008)

$$N_1 = \frac{27}{4} \left(\frac{1}{1-\phi} \right) k_\omega$$

$$Y_{RT}^s = 0.87 Y_{RT}$$
$$R_d^s = 0.92 R_d$$
$$N_1 = 54$$
$$k_\omega \sim 8$$

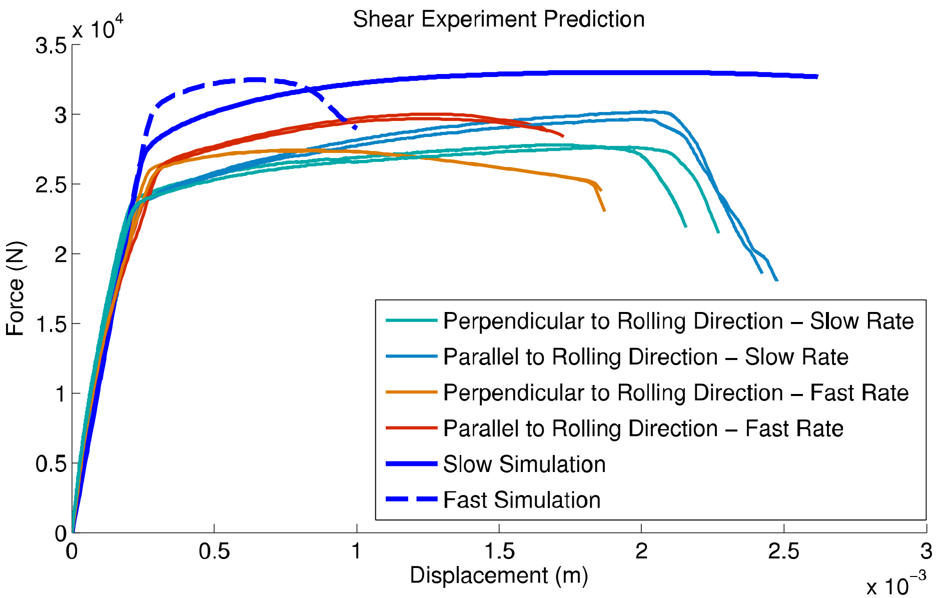

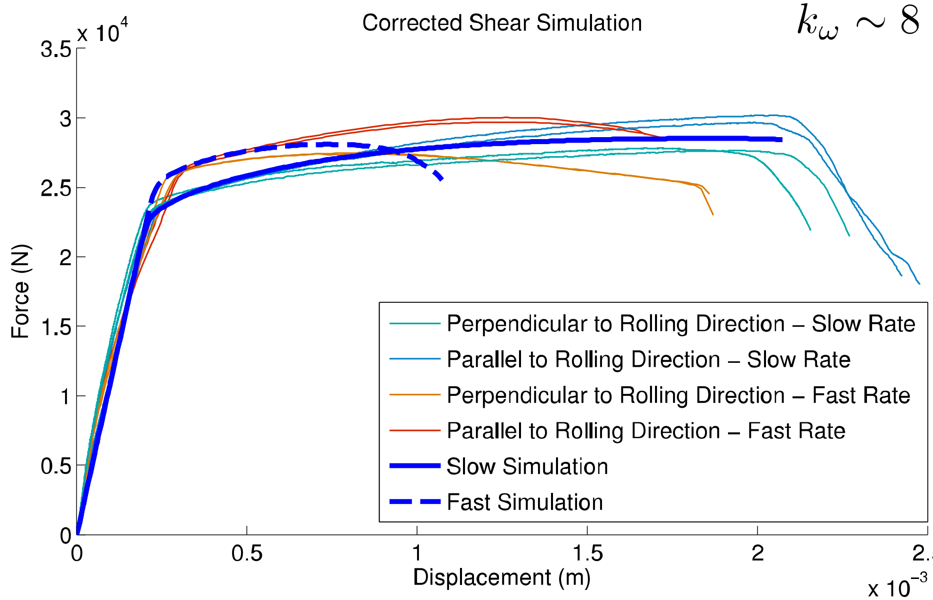

Revised approach to SFC geometry

- Calibrated a Hill, anisotropic yield surface to the shear and tensile data
- Although rate and temperature independent, modest agreement at lower rates
- Anisotropic yield predicted SFC would localize in the lower notch

Idealization. Keep poro-thermo-viscoplasticity. Accept isotropy. Assign different isotropic material parameters to regions being sheared.

Goal. Mimic Hill at lower notch, add physics

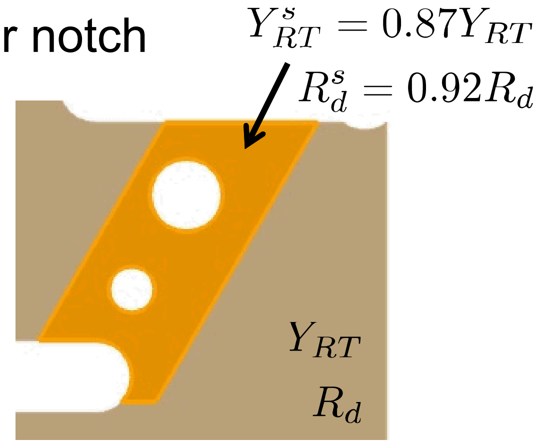

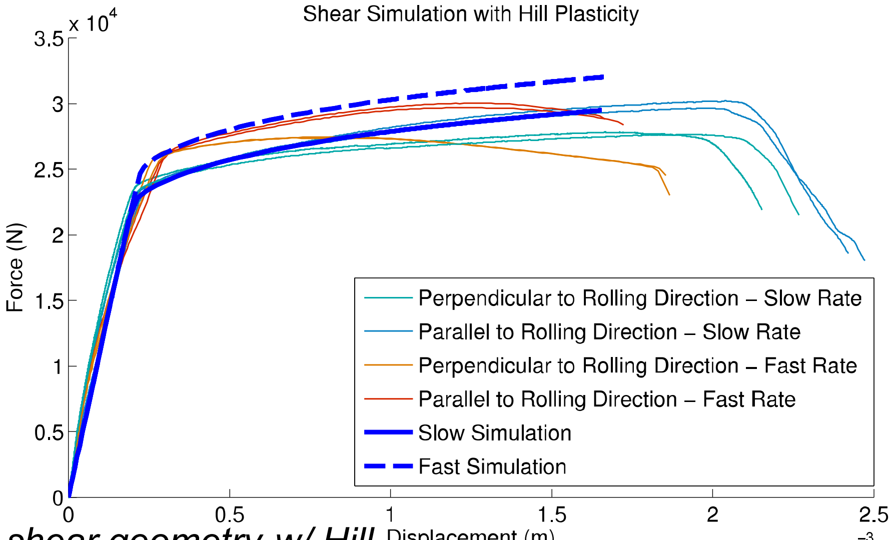

shear geometry w/ Hill

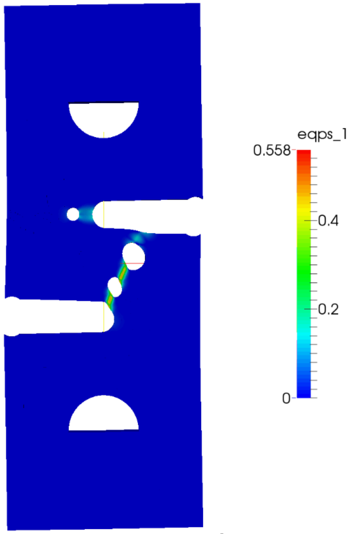

SFC geometry w/Hill

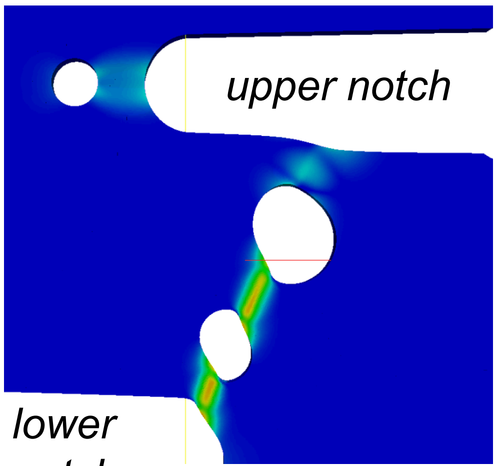

SFC w/Hill

Blind predictions

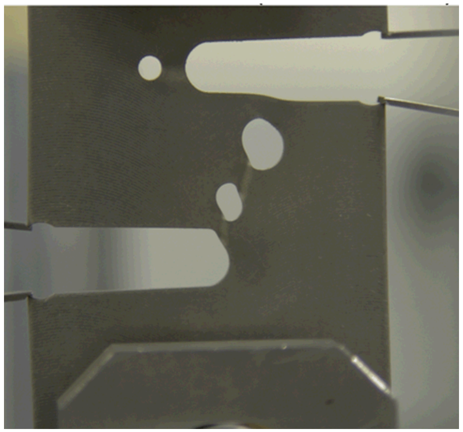

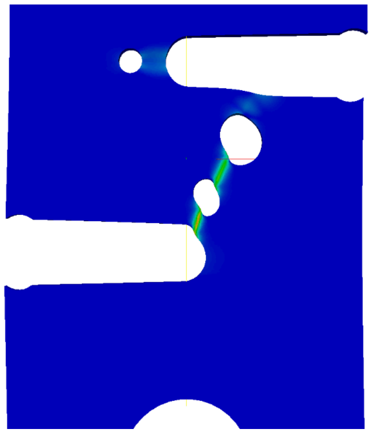

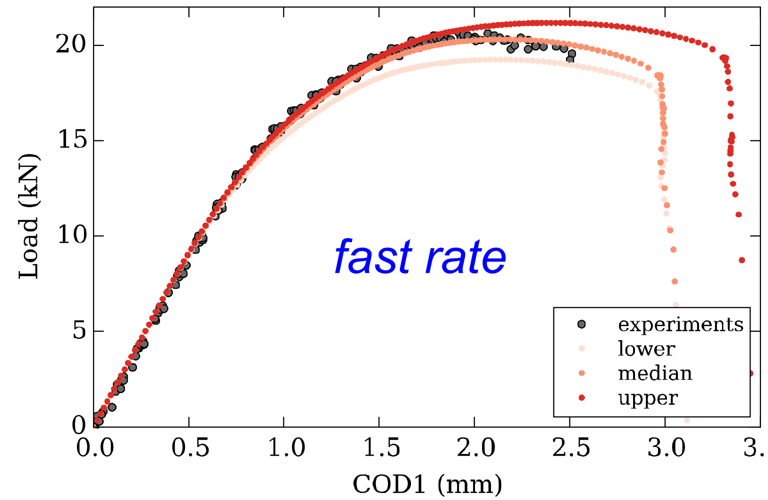

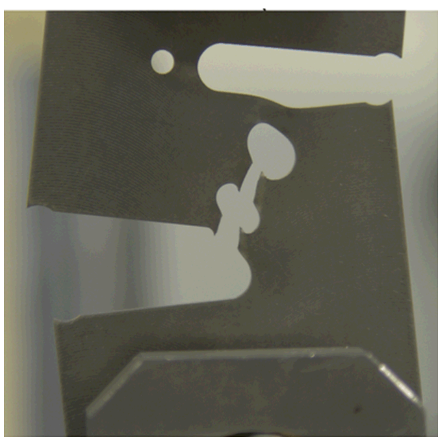

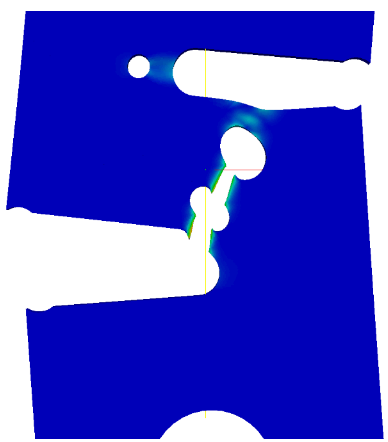

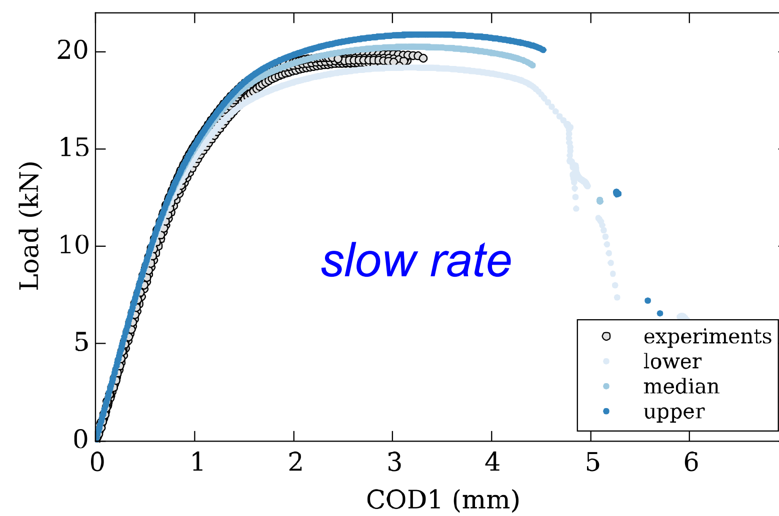

In good company…

- Majority of teams predicted the correct crack path w/error in load-displacement
- Majority of teams over-predicted both the loads and displacements to failure
- We believed that the role of plastic anisotropy would improve our predictions

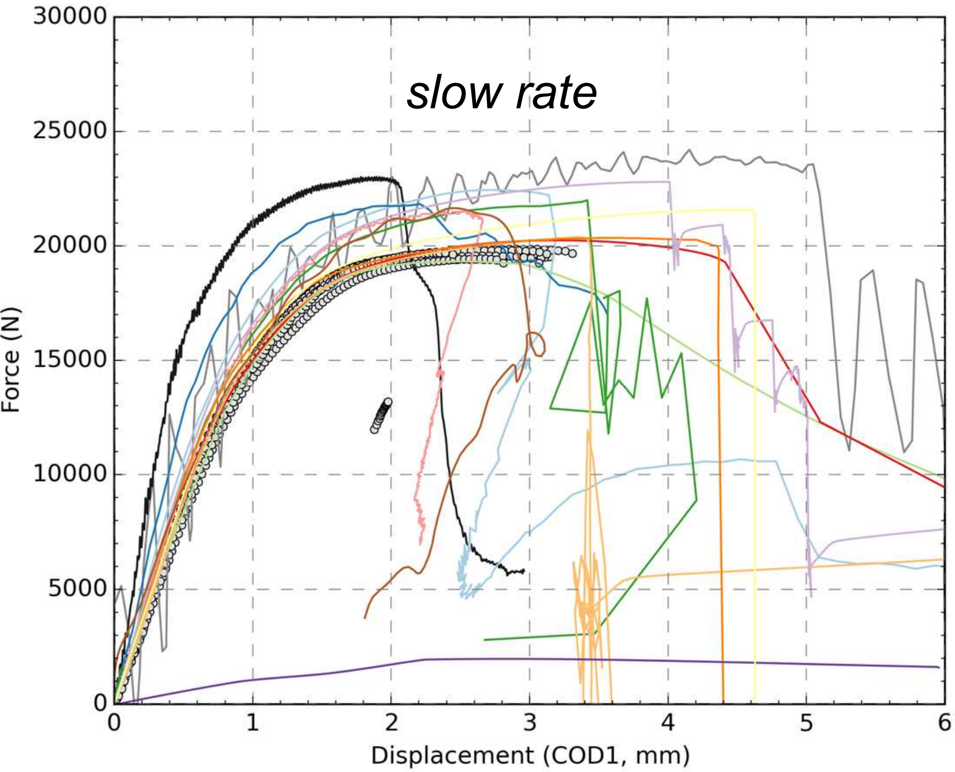

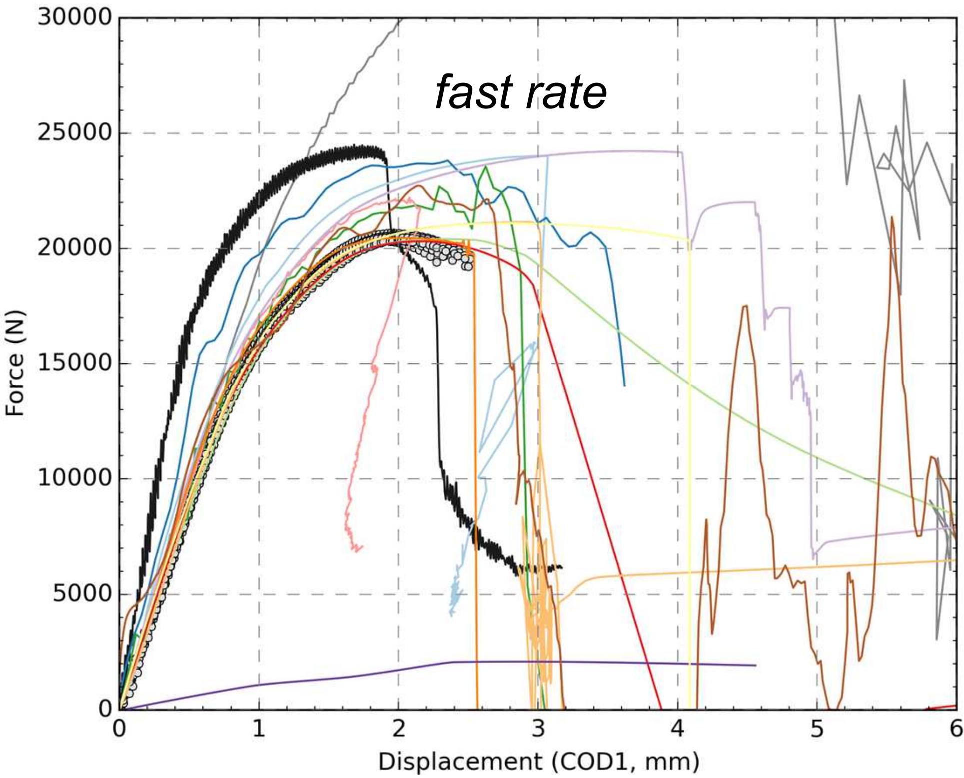

Sensitivity studies

thermal parameter, β

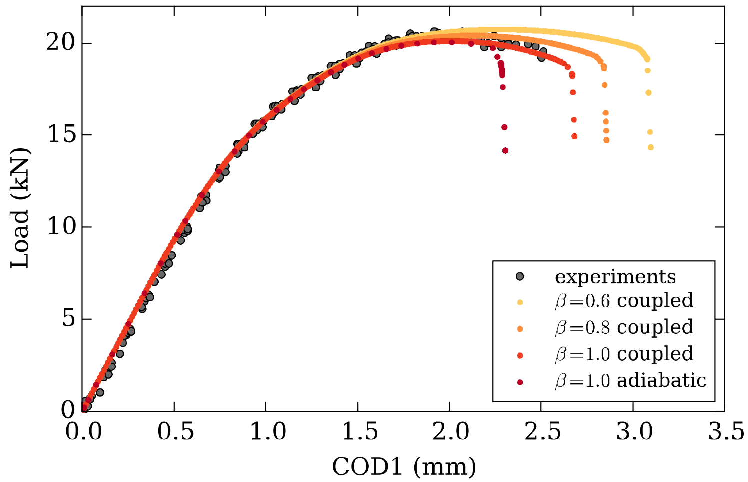

void growth damage, m

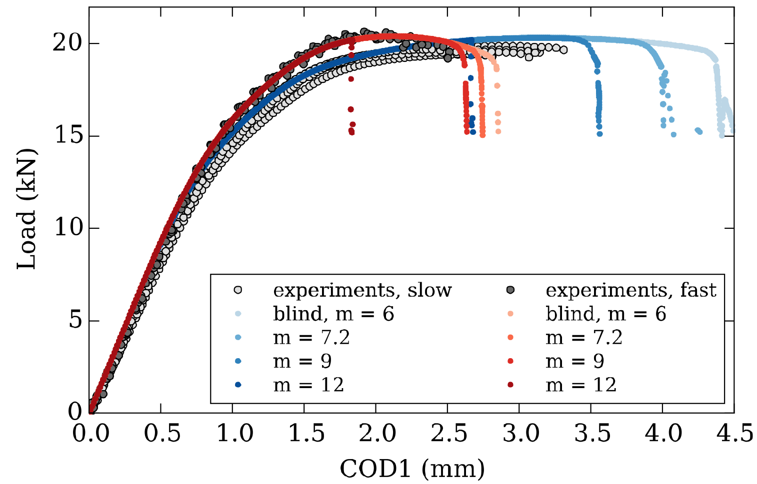

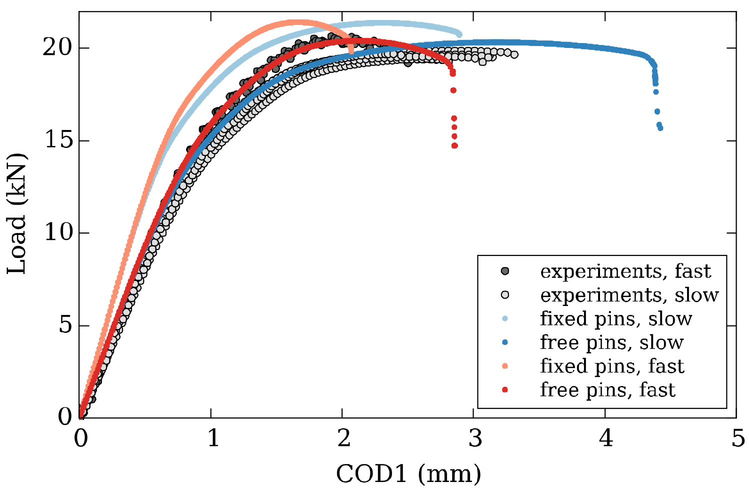

pin boundary condition

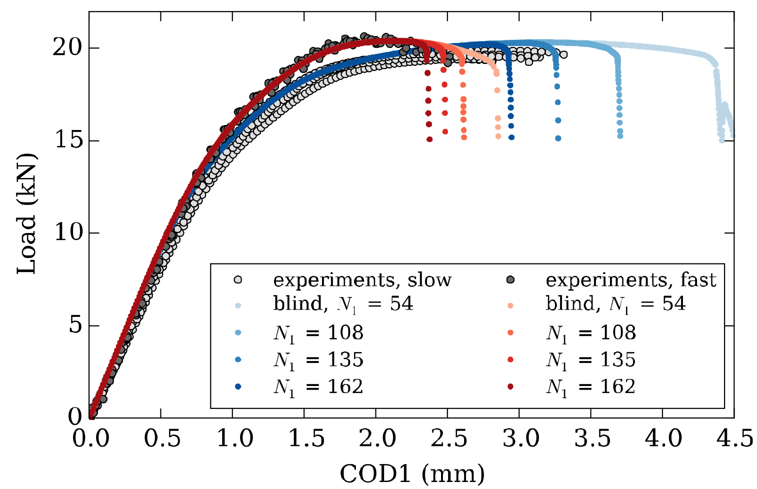

Void nucleation damage, N1

Revisiting anisotropy

- Keep micromechanics (damage)
- Add Hill yield surface
- Aids understanding

$$\dot{\phi} = \sqrt{\frac{3}{2}}\dot{\epsilon}_p \frac{1-(1-\phi)^{m+1}}{(1-\phi)^m} \sinh\left[\frac{2(2m-1)}{2m+1}\frac{\langle \frac{I_1}{3}\rangle}{\sqrt{3J_2}}\right]$$

$$\dot{\eta} = \eta\dot{\epsilon}_p N_1 \left[\frac{4}{27} - \frac{J_3^2}{J_2^3}\right]$$

$$f_Y^2(\sigma_{ij}) \equiv F(\sigma_{22}-\sigma_{33})^2 + G(\sigma_{33}-\sigma_{11})^2 + H(\sigma_{11}-\sigma_{22})^2 + 2L\sigma_{23}^2 + 2M\sigma_{31}^2 + 2N\sigma_{12}^2 = \bar{\sigma}_c^2(\epsilon_p)$$

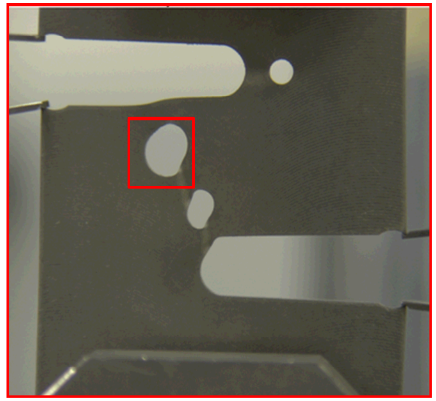

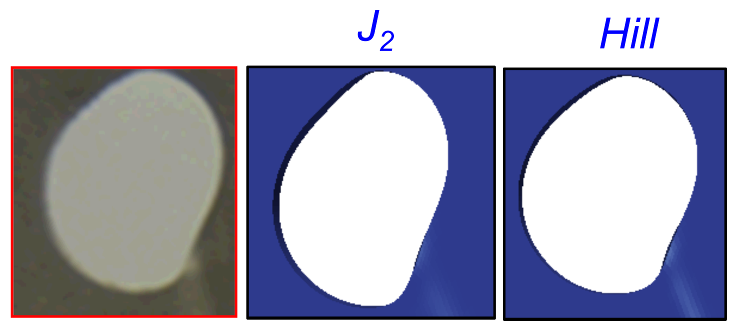

hole elongation reflects anisotropy

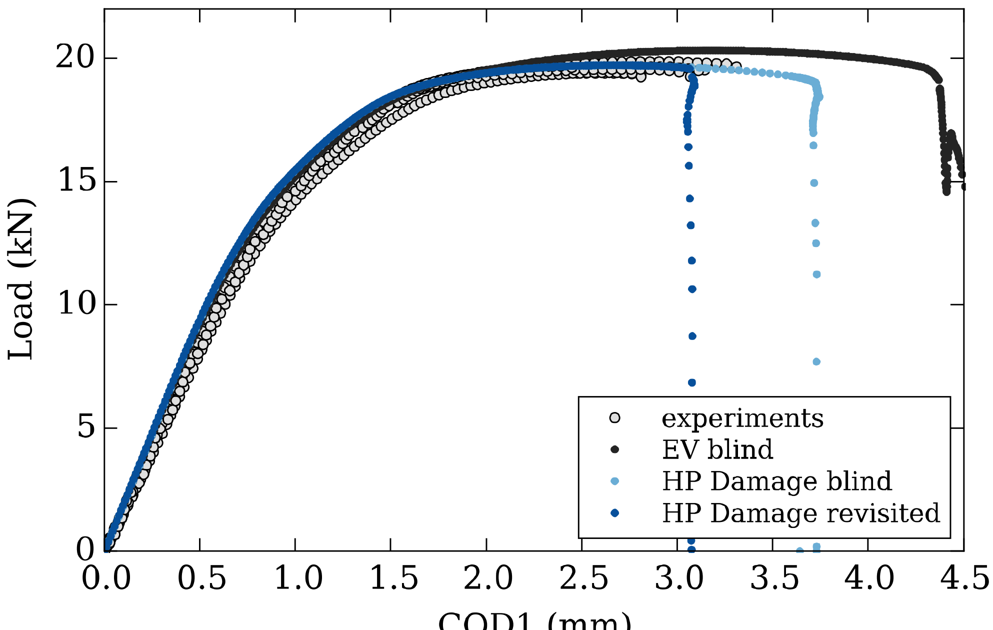

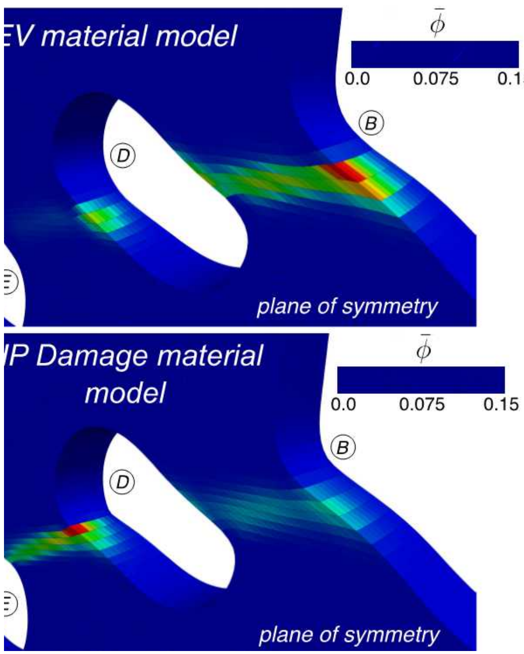

Ravi-Chandar Gross (UT)

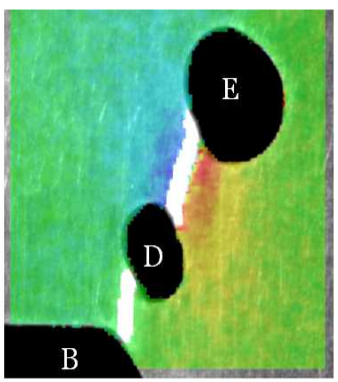

Revisiting regularization

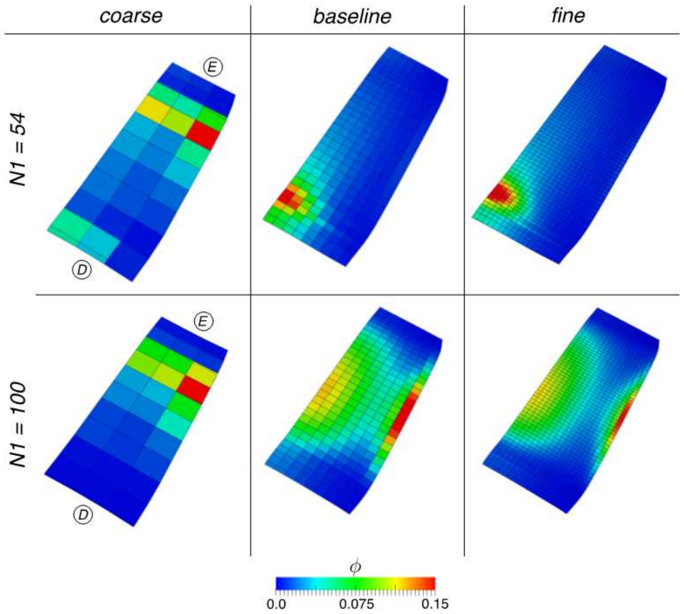

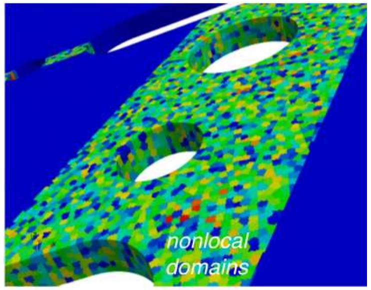

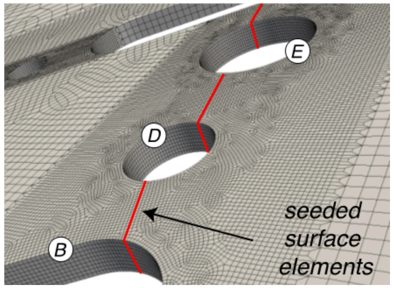

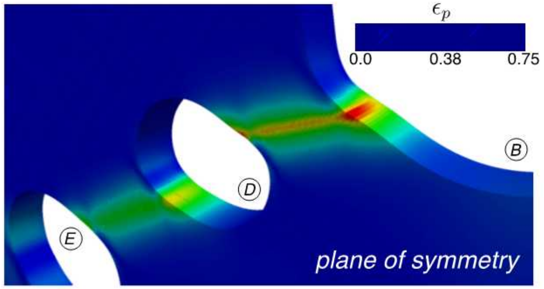

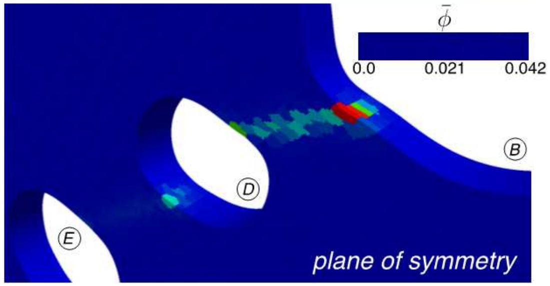

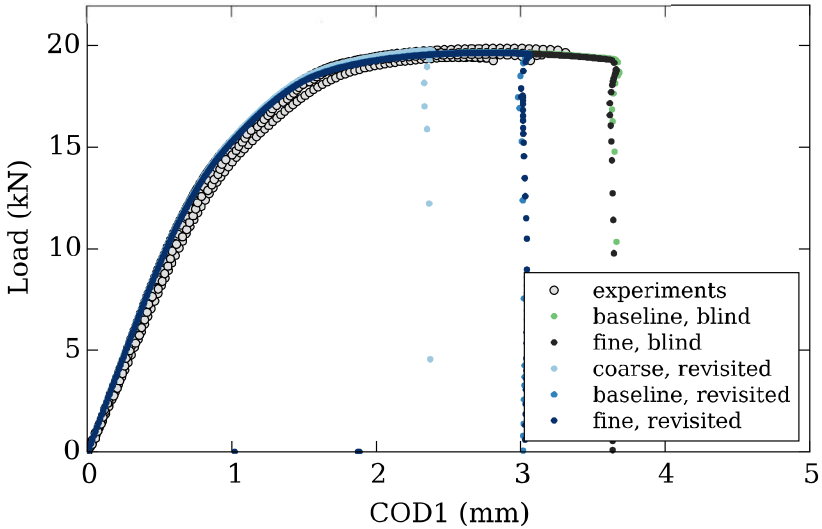

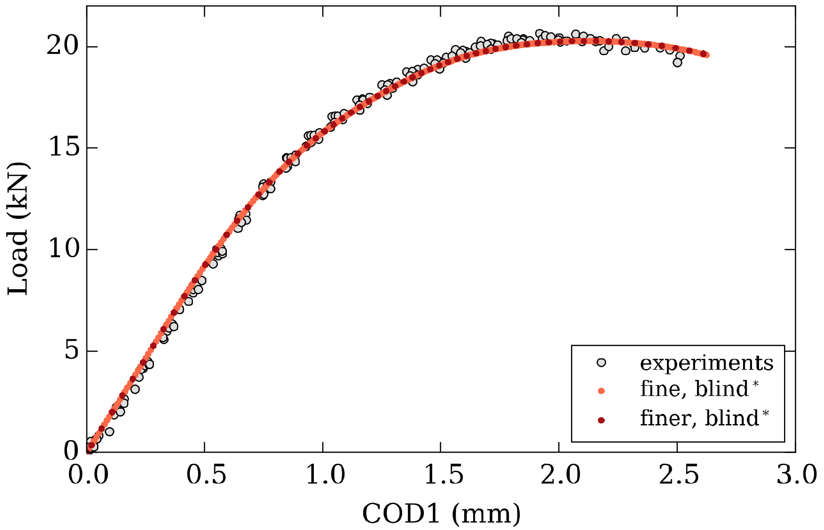

304L laser welds provide motivation

Surface observations indicate that the failure of 304-L is a primarily a necking process. Interrupted testing will determine the role of crack initiation.

Hypothesis: Pore size and distribution can aid the necking process and crack initiation

- μ-CT needed to probe initial and interrupted pore structures
- Remeshing/mapping needed to resolve the evolution of pore structure
- Homogenization not applicable

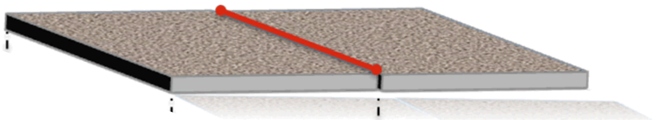

304-L butt weld

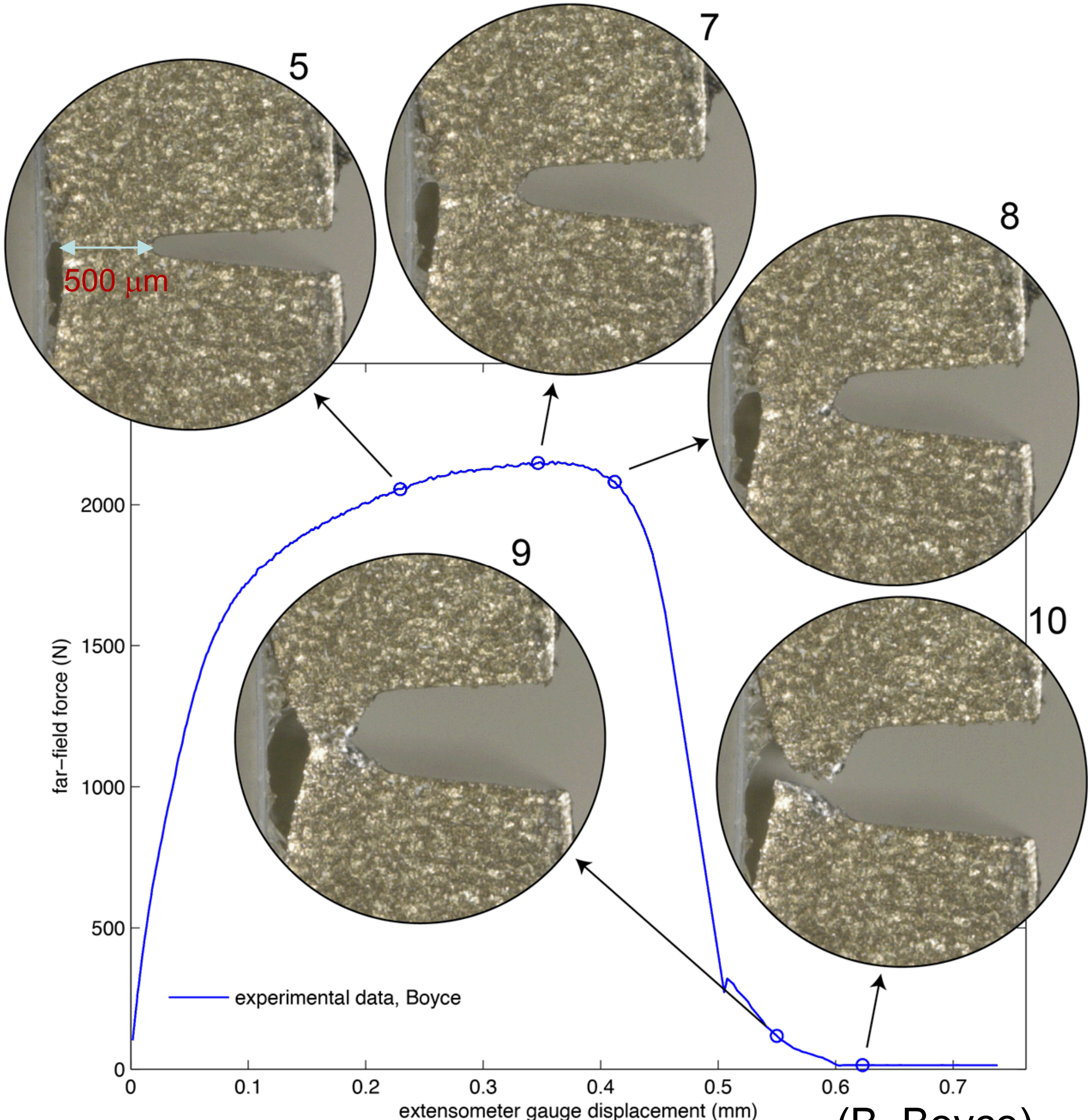

(B. Boyce)

Deeper welds galvanize efforts

Weld schedule impacts porosity. Porosity impacts performance.

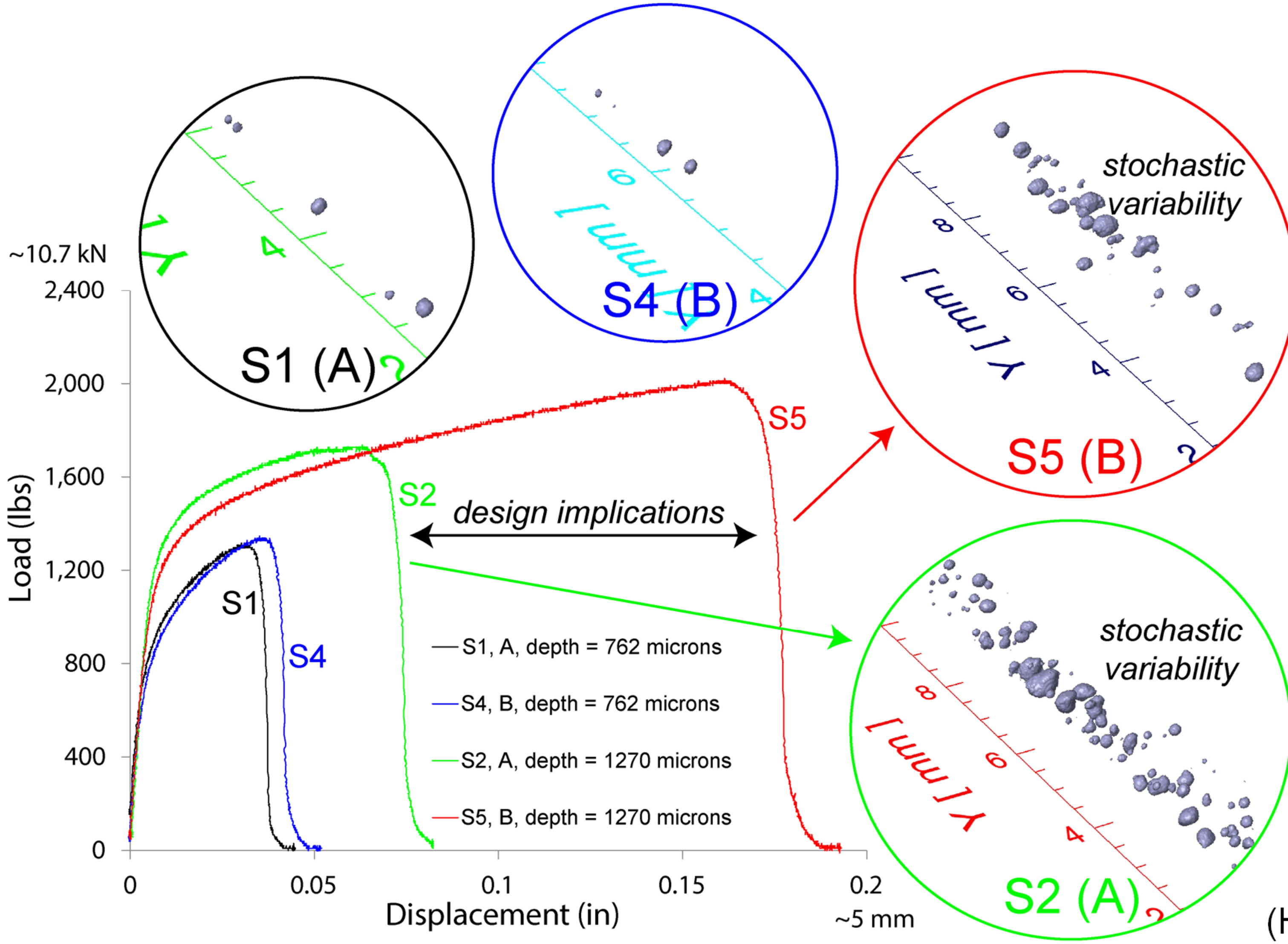

(H. Jin, J. Madison)

10-Node Composite Tetrahedral Element

Motivated by prior work of Thoutireddy, et. al., IJNME (2002)

$$\Phi[\boldsymbol{\varphi}, \bar{\boldsymbol{F}}, \bar{\boldsymbol{P}}] := \int_B A(\bar{\boldsymbol{F}})\,\mathrm{d}V + \int_B \bar{\boldsymbol{P}} : (\boldsymbol{F} - \bar{\boldsymbol{F}})\,\mathrm{d}V - \int_B R\boldsymbol{B} \cdot \boldsymbol{\varphi}\,\mathrm{d}V - \int_{\partial_T B} \boldsymbol{T} \cdot \boldsymbol{\varphi}\,\mathrm{d}S$$

$$\bar{\boldsymbol{P}} = \lambda_\alpha \left(\int_\Omega \lambda_\alpha \lambda_\beta \boldsymbol{I}\,\mathrm{d}V \right)^{-1} \int_\Omega \lambda_\beta \boldsymbol{P}\,\mathrm{d}V,$$

$$\bar{\boldsymbol{F}} = \lambda_\alpha \left(\int_\Omega \lambda_\alpha \lambda_\beta \boldsymbol{I}\,\mathrm{d}V \right)^{-1} \int_\Omega \lambda_\beta \boldsymbol{F}\,\mathrm{d}V$$

$$\boldsymbol{R}_a(\boldsymbol{\varphi}) := \int_\Omega \bar{\boldsymbol{P}} \cdot \boldsymbol{\mathcal{B}}_a\,\mathrm{d}V - \int_\Omega R\boldsymbol{B} N_a\,\mathrm{d}V - \int_{\partial_T \Omega} \boldsymbol{T} N_a\,\mathrm{d}S = \boldsymbol{0}$$

$$\boldsymbol{\mathcal{B}}_a(\boldsymbol{X}) := \delta_{ik} \frac{\partial N_a(\boldsymbol{X})}{\partial X_J}\, \boldsymbol{e}_i \otimes \boldsymbol{E}_J \otimes \boldsymbol{e}_k$$

- $\boldsymbol{\varphi}$ — C^0 piecewise linear
- $\bar{\boldsymbol{F}}$ — C^{-1} linear over parent element
- $\bar{\boldsymbol{P}}$ — C^{-1} linear over parent element

12 sub-tets

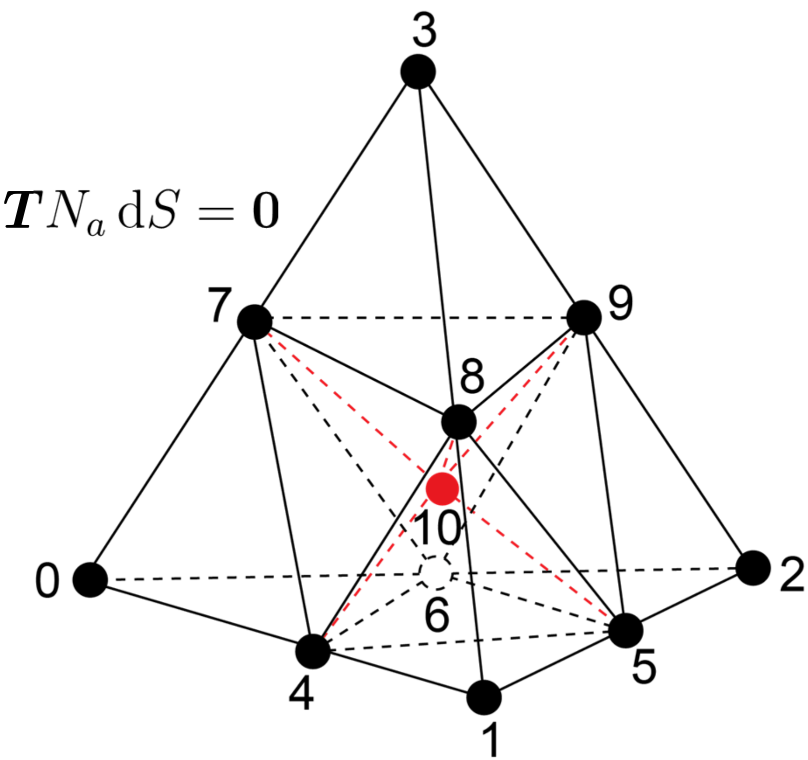

Analytical gradient operator

Develop an exact gradient operator that projects and interpolates sub-tet gradients

$$\bar{\boldsymbol{F}}(\boldsymbol{X}) := \bar{\boldsymbol{\mathcal{B}}}_a(\boldsymbol{X})\boldsymbol{x}_a$$

$$\bar{\boldsymbol{\mathcal{B}}}_a(\boldsymbol{X}) := \lambda_\alpha(\boldsymbol{X})\left[\int_\Omega \delta_{ik}\lambda_\alpha(\boldsymbol{X})\lambda_\beta(\boldsymbol{X})\,\mathrm{d}V\right]^{-1}\int_\Omega \lambda_\beta(\boldsymbol{X})\frac{\partial N_a(\boldsymbol{X})}{\partial X_J}\,\mathrm{d}V\,\boldsymbol{e}_i\otimes\boldsymbol{E}_J\otimes\boldsymbol{e}_k$$

$$\bar{\boldsymbol{\mathcal{B}}}_a(\boldsymbol{\xi}) = \lambda_\alpha(\boldsymbol{\xi})\left[\int_{\Omega_{\boldsymbol{\xi}}} \delta_{ik}\lambda_\alpha(\boldsymbol{\xi})\lambda_\beta(\boldsymbol{\xi})\,\mathrm{d}V_{\boldsymbol{\xi}}\right]^{-1}\int_{\Omega_{\boldsymbol{\xi}}} \lambda_\beta(\boldsymbol{\xi})\frac{\partial N_a(\boldsymbol{\xi})}{\partial \boldsymbol{\xi}}\,\mathrm{d}V_{\boldsymbol{\xi}}\left(\frac{\partial \boldsymbol{\xi}}{\partial X_J}\right)\boldsymbol{e}_i\otimes\boldsymbol{E}_J\otimes\boldsymbol{e}_k$$

$$\bar{\boldsymbol{\mathcal{B}}}_a(\boldsymbol{\xi}) = \bar{\mathcal{L}}_{a;ilk}(\boldsymbol{\xi})\left(\frac{\partial \xi_l}{\partial X_J}\right)\boldsymbol{e}_i\otimes\boldsymbol{E}_J\otimes\boldsymbol{e}_k$$

$$\bar{\boldsymbol{\mathcal{L}}}_a(\boldsymbol{\xi}) = \lambda_\alpha(\boldsymbol{\xi})\delta_{ik}(M_{\alpha\beta})^{-1}\sum_{S=0}^{11}\frac{\partial N_a}{\partial \xi_l}\int_{E_S}\lambda_\beta(\boldsymbol{\xi})\,\mathrm{d}V_{\boldsymbol{\xi}}\,\boldsymbol{e}_i\otimes\boldsymbol{a}_l\otimes\boldsymbol{e}_k$$

$$\bar{\boldsymbol{\mathcal{B}}}_a(\boldsymbol{\xi}) = \bar{\mathcal{L}}_{a;ilk}(\boldsymbol{\xi})\left[\bar{\mathcal{L}}_{b;JlM}(\boldsymbol{\xi})X_{b;M}\right]^{-1}\boldsymbol{e}_i\otimes\boldsymbol{E}_J\otimes\boldsymbol{e}_k$$

$$\bar{B}_{aJ}(\boldsymbol{\xi}) = \bar{L}_{al}(\boldsymbol{\xi})\left[X_{Jb}\bar{L}_{bl}(\boldsymbol{\xi})\right]^{-1}$$

$$\bar{F}_{iJ}(\boldsymbol{\xi}) = x_{ia}\bar{B}_{aJ}(\boldsymbol{\xi})$$

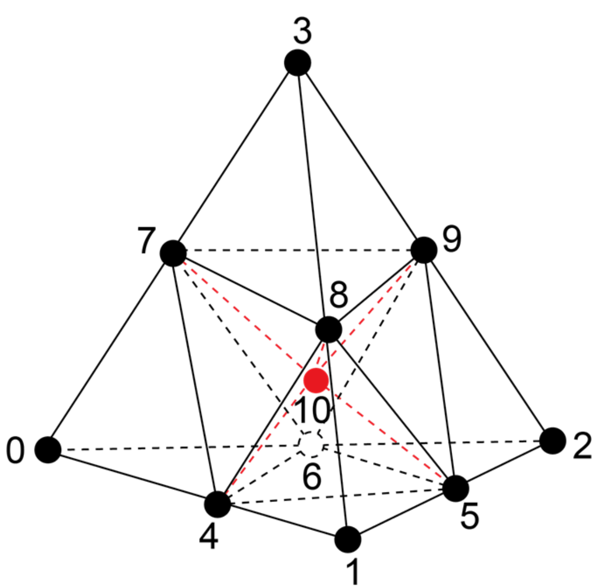

$$\bar{L}_{al}(\boldsymbol{\xi}) \equiv \bar{L}_{10\times 3} = \frac{1}{24}\begin{pmatrix} 9-60\xi_0 & 9-60\xi_0 & 9-60\xi_0 \\ -9+60\xi_1 & 0 & 0 \\ 0 & -9+60\xi_2 & 0 \\ 0 & 0 & -9+60\xi_3 \\ 70(\xi_0-\xi_1) & 2(-4-35\xi_1+5\xi_2+10\xi_3) & 2(-4-35\xi_1+10\xi_2+5\xi_3) \\ 2(-1+5\xi_1+40\xi_2-5\xi_3) & 2(-1+40\xi_1+5\xi_2-5\xi_3) & 10(\xi_0-\xi_3) \\ 2(-4+5\xi_1-35\xi_2+10\xi_3) & 70(\xi_0-\xi_2) & 2(-4+10\xi_1-35\xi_2+5\xi_3) \\ 2(-4+5\xi_1+10\xi_2-35\xi_3) & 2(-4+10\xi_1+5\xi_2-35\xi_3) & 70(\xi_0-\xi_3) \\ 2(-1+5\xi_1-5\xi_2+40\xi_3) & 10(\xi_0-\xi_2) & 2(-1+40\xi_1-5\xi_2+5\xi_3) \\ 10(\xi_0-\xi_1) & 2(-1-5\xi_1+5\xi_2+40\xi_3) & 2(-1-5\xi_1+40\xi_2+5\xi_3) \end{pmatrix}.$$

Evaluate for your integration scheme

Suitable for isochoric motions

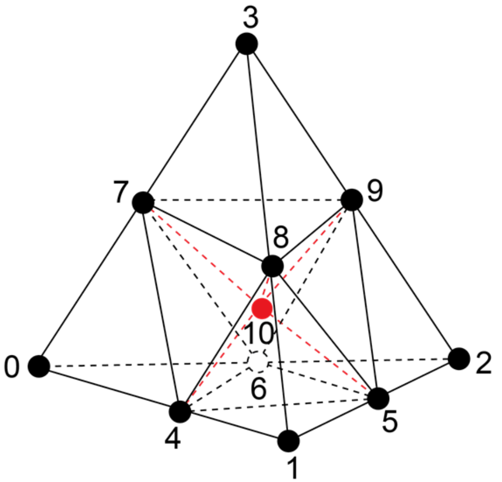

Volume-averaged formulation does not exhibit spurious pressure oscillations.

$$\bar{\boldsymbol{F}}^{\star}(\boldsymbol{\xi}) := \left(\frac{\bar{J}^{\star}}{\bar{J}(\boldsymbol{\xi})}\right)^{\frac{1}{3}} \bar{\boldsymbol{F}}(\boldsymbol{\xi})$$

$$\bar{J}^{\star} := \frac{\int_{\Omega} \bar{J} \, \mathrm{d}V}{\int_{\Omega} \mathrm{d}V}$$

$$\bar{p}^{\star} := \frac{1}{V_{\Omega}} \int_{\Omega} \mathrm{tr} \, \frac{\partial A(\boldsymbol{F}^{\star})}{\partial \bar{\boldsymbol{b}}^{\star}} \, \mathrm{d}V$$

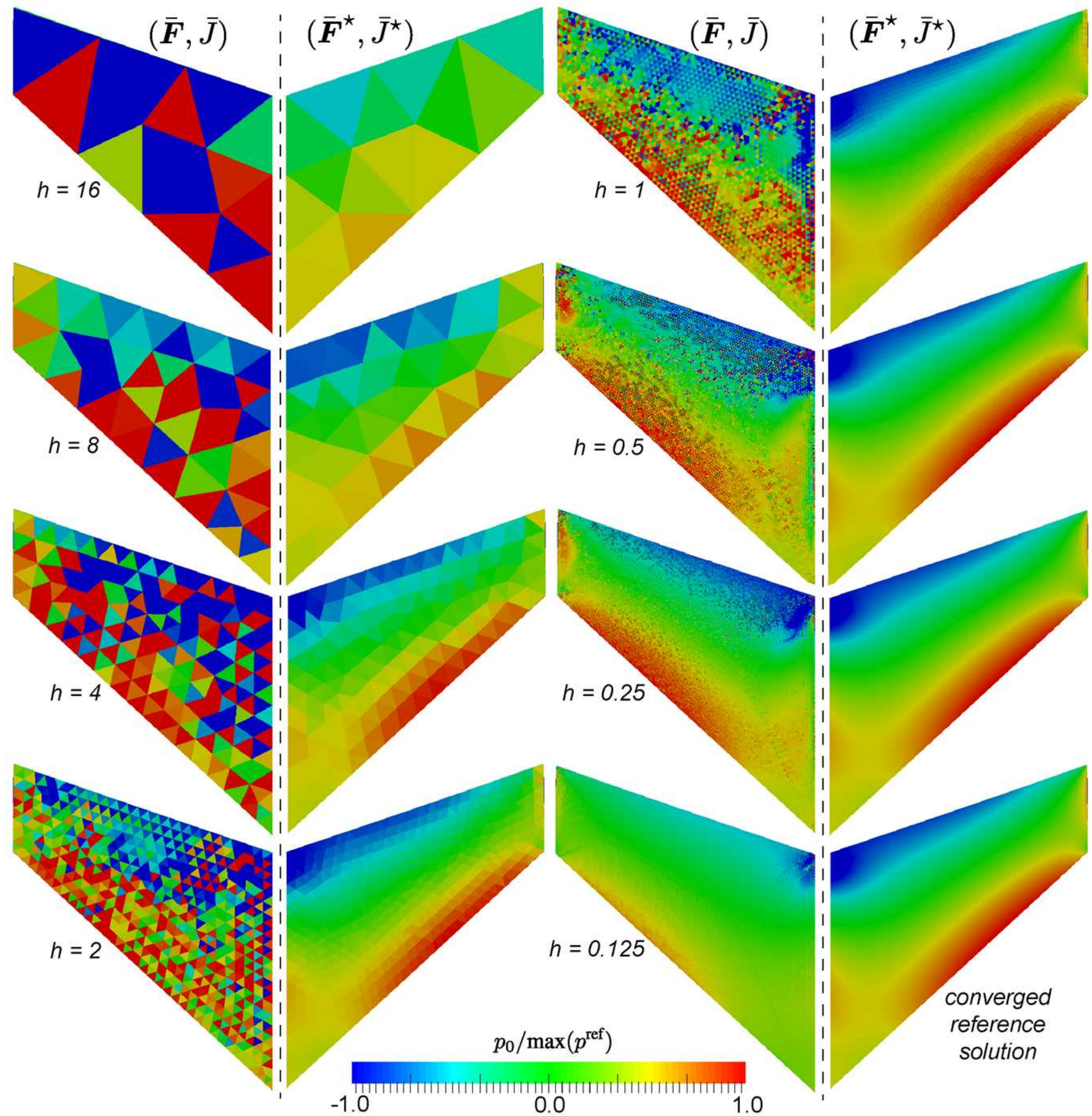

mapLL (L_2 + Lie Group/Algebra)

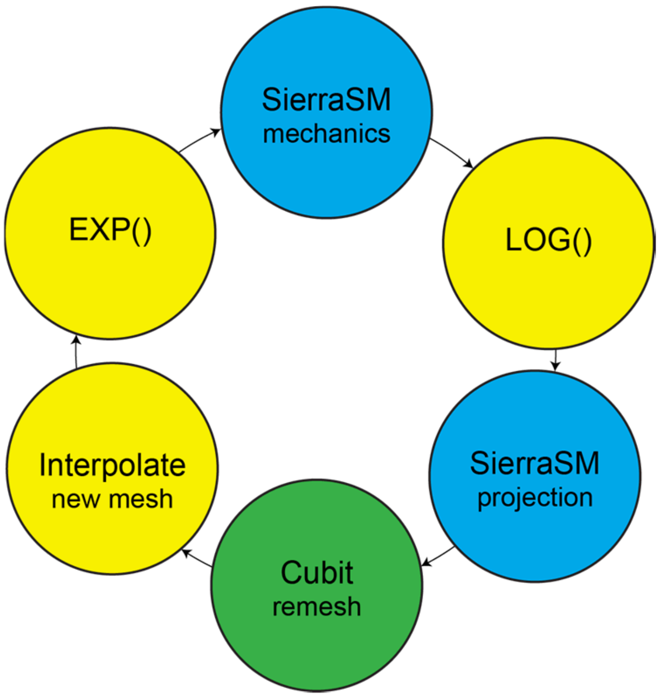

$$\Phi[\boldsymbol{\varphi}, \bar{\boldsymbol{z}}, \bar{\boldsymbol{y}}] := \int_B W(\boldsymbol{F}, \bar{\boldsymbol{z}})\, dV + \int_B \bar{\boldsymbol{y}} \cdot (\bar{\boldsymbol{z}} - \boldsymbol{z})\, dV - \int_B \rho_0 \boldsymbol{B} \cdot \boldsymbol{\varphi}\, dV - \int_{\partial_T B} \boldsymbol{T} \cdot \boldsymbol{\varphi}\, dS$$

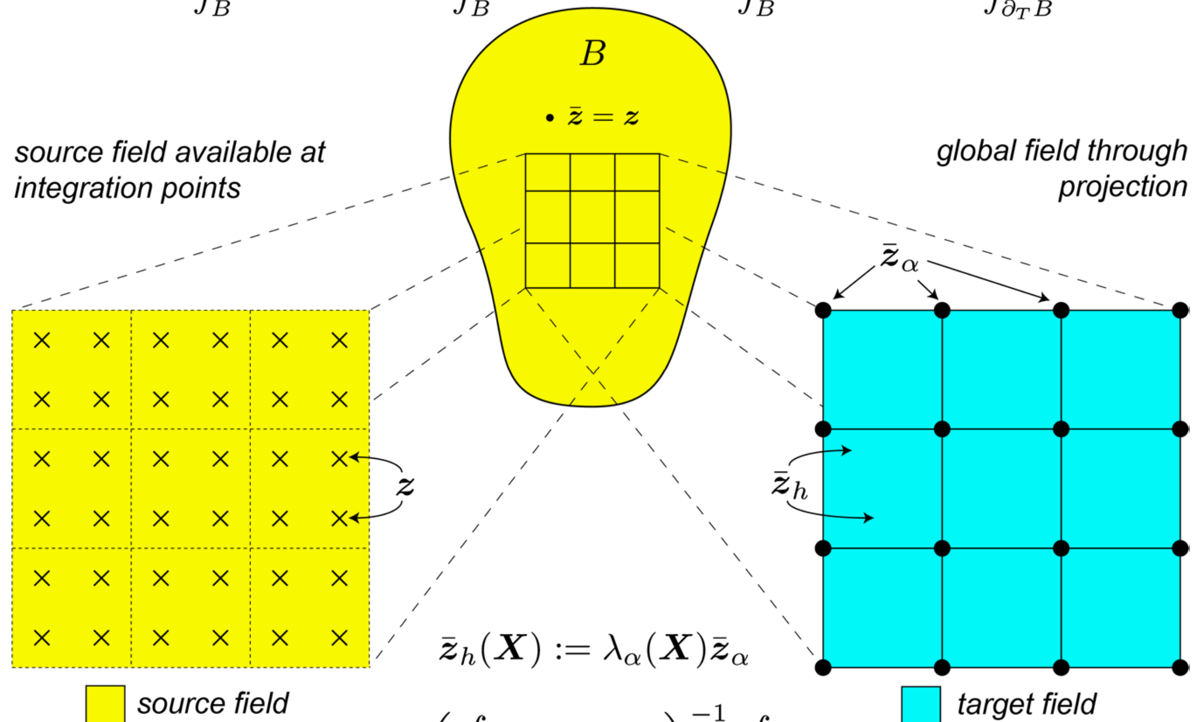

$$\bar{\boldsymbol{z}}_h = \lambda_\alpha \left(\int_B \lambda_\alpha \lambda_\beta \boldsymbol{I}\, dV \right)^{-1} \int_B \lambda_\beta \boldsymbol{z}\, dV$$

- The variational principle naturally yields an optimal, L_2 projection
- The spaces of variables (Lie algrebra, Lie Group) are honored through log() and exp()
- Advocated by Mota, et. al., Computational Mechanics, 2013

  Past works: Ortiz and Quigley (1991), Camacho and Ortiz (1997), Radovitzky and Ortiz (1999), Rashid (2002), Jiao and Heath (2004)

Adopting a new reference

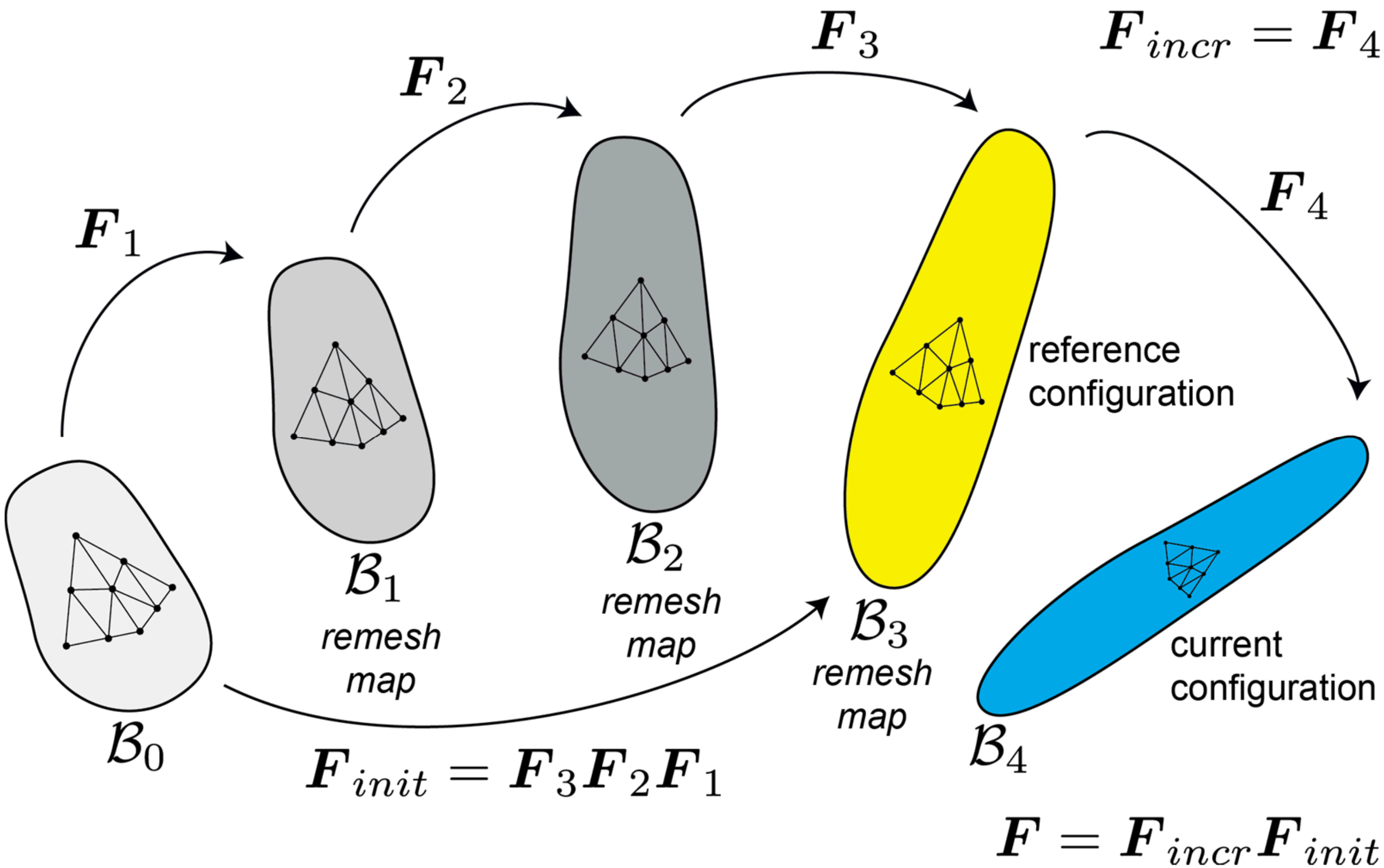

- Prior work on hexahedral elements maintained the reference configuration
- Elements degrade in the reference configuration - T-L element integrate in reference
- We now adopt a new reference configuration and map $\mathbf{F}_{init}$ (which lives in a Lie Group)

Mapping procedure

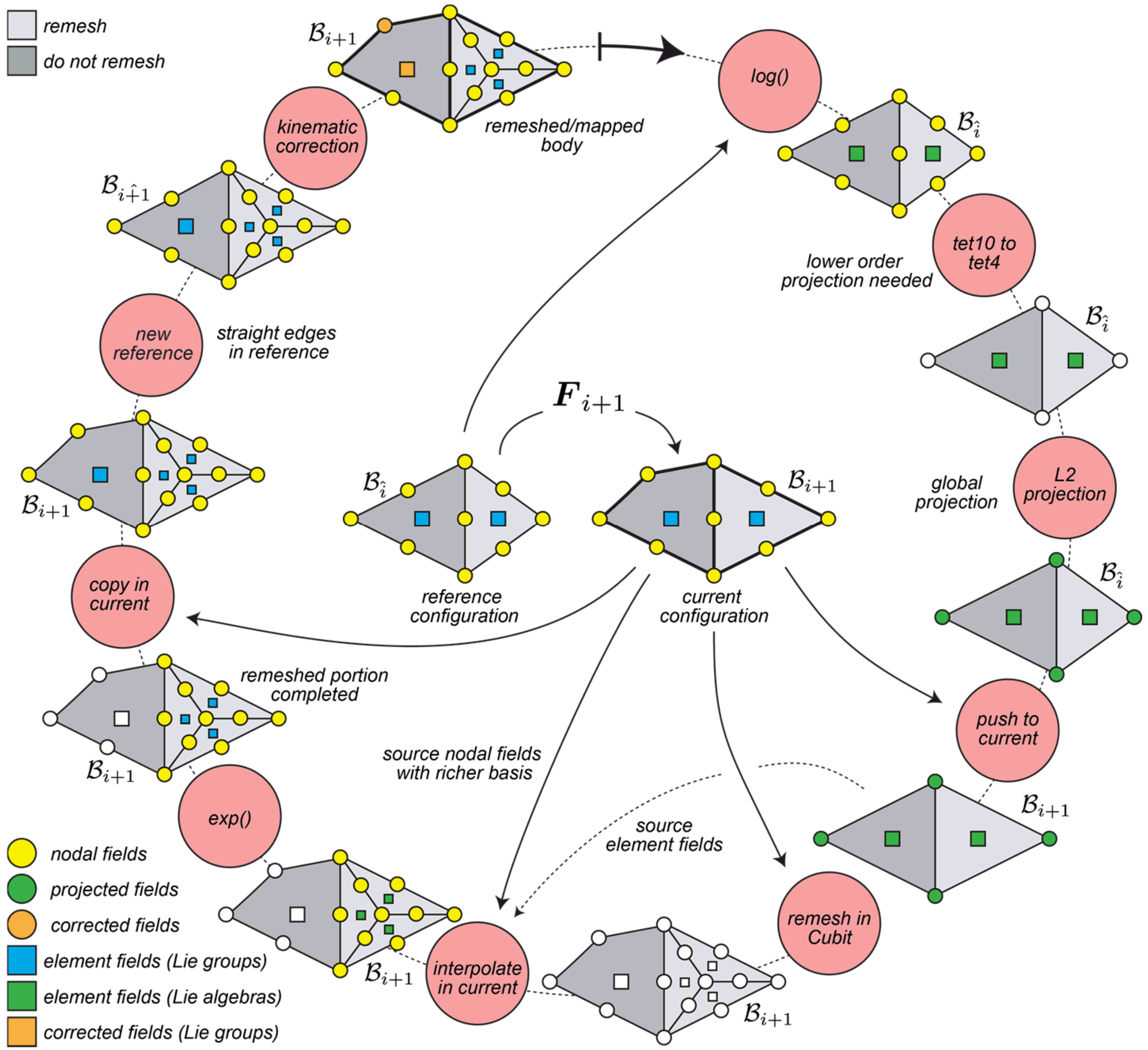

Remeshing/mapping discrete pores

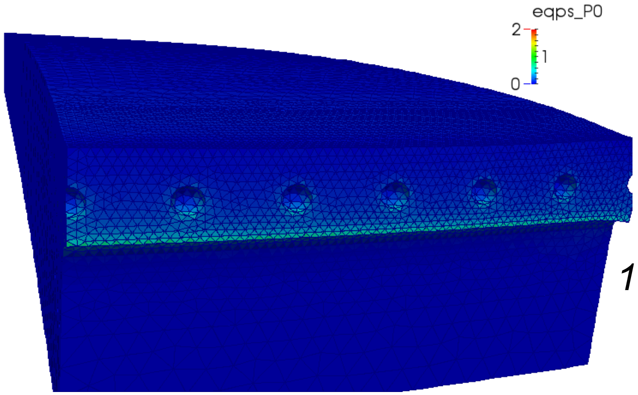

1st map

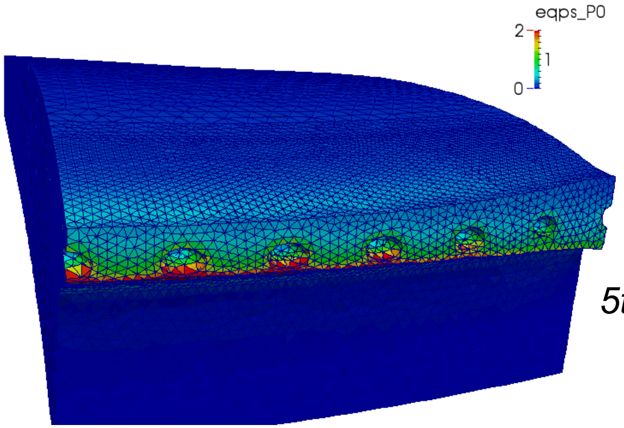

5th map

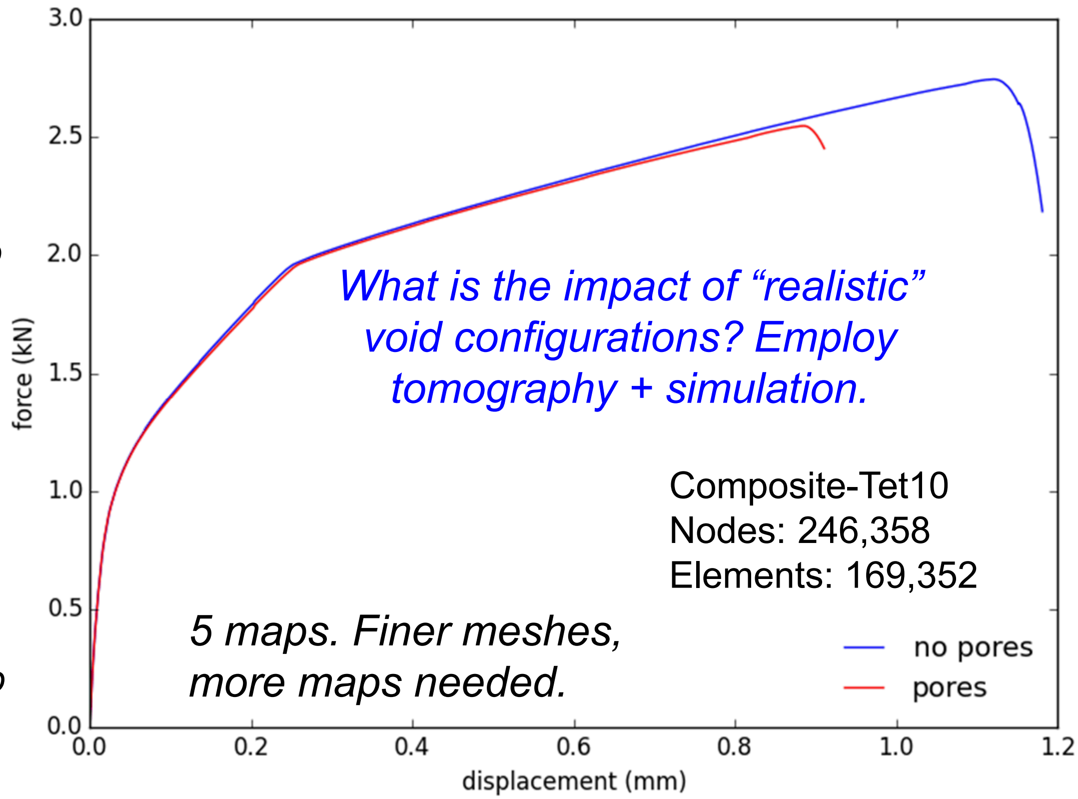

What is the impact of "realistic" void configurations? Employ tomography + simulation.

Composite-Tet10
Nodes: 246,358
Elements: 169,352

5 maps. Finer meshes, more maps needed.

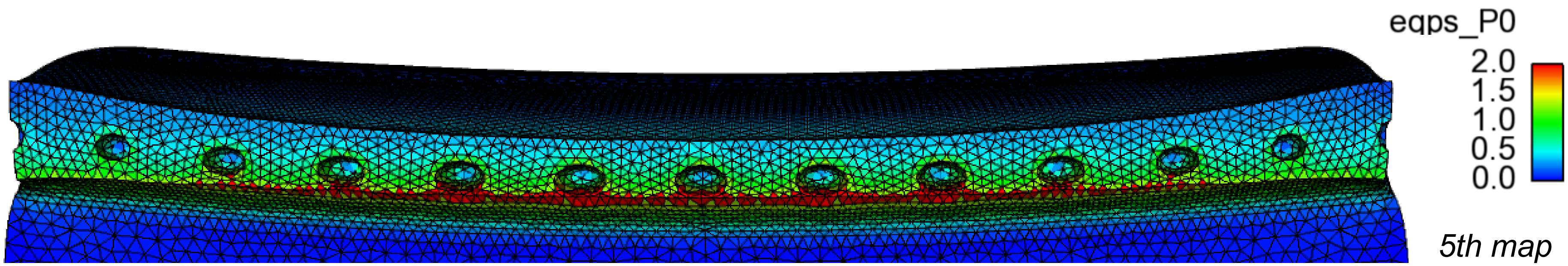

5th map

Additional views of necking process

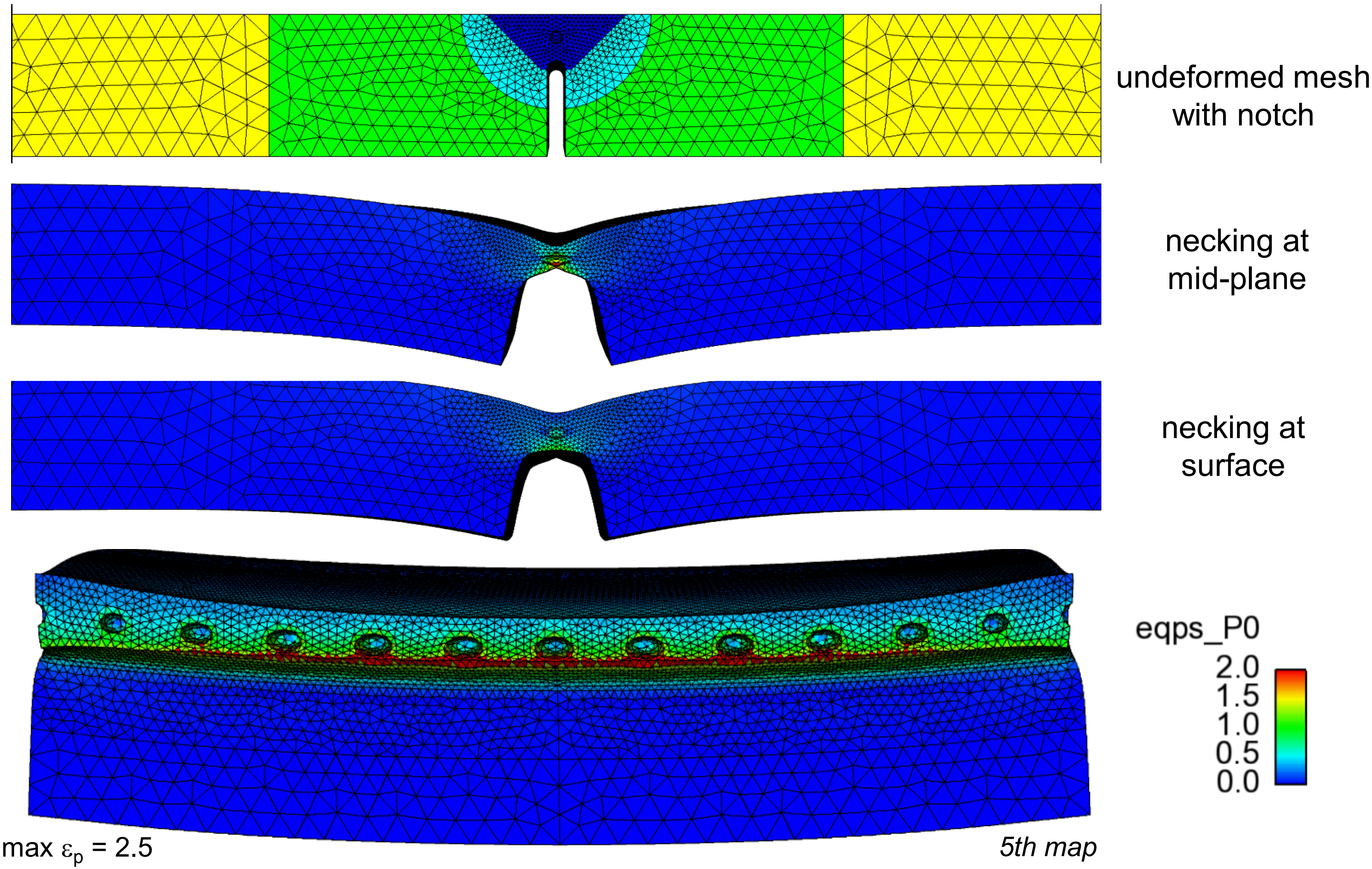

Increasing the number of mappings

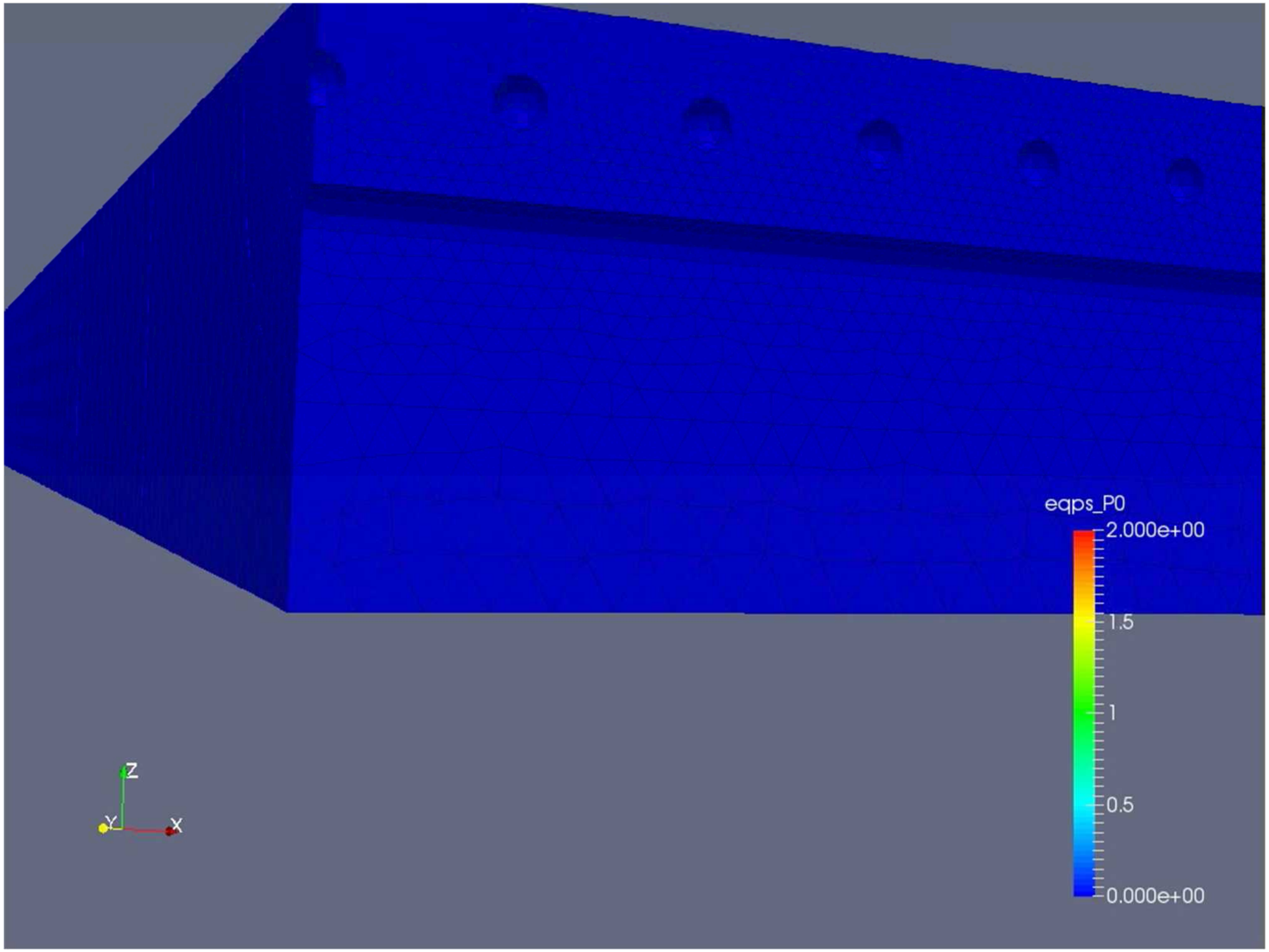

Reflections and path forward

- Refocused task
  - Hardening nonlocality and localization elements
  - Physics drive localization – investing in constitutive modeling
  - Documenting work on optimal meshes/bifurcation
  - Emphasizing linkage to SierraSM and X-FEM
- Illustrated blind and revisited SFC2 predictions
  - Importance of coupling, rate dependence, anisotropy, and nucleation
  - Regularized physics with multiple methodologies
- Highlighted work in remeshing/mapping of internal state variables
  - Massive deformations often accompany the localization process
  - Proposed methodology resolves inelasticity to strains in excess of 6
  - Composite tetrahedral element technology complements adaptivity